AGU PUBLICATIONS

JGR

Journal of Geophysical Research: Biogeosciences

RESEARCH ARTICLE
10.1002/2015JG003163

Key Points:
- First modern time-series-coupled upwelling and biogeochemical study in the southeastern Arabian Sea
- The 2012 shelf oxygen levels are similar to 1958–1960 except marginal variation during peak upwelling
- Despite shifts in seasonal trophic status, the inner shelf system exhibited annual net autotrophy

Supporting Information:
- Supporting Information S1

Correspondence to:
G. V. M. Gupta,
gvmgupta@cmlre.gov.in;
gvmgupta@gmail.com

Citation:
Gupta, G. V. M., V. Sudheesh, K. V. Sudharma, N. Saravanane, V. Dhanya, K. R. Dhanya, G. Lakshmi, M. Sudhakar, and S. W. A. Naqvi (2016), Evolution to decay of upwelling and associated biogeochemistry over the southeastern Arabian Sea shelf, *J. Geophys. Res. Biogeosci.*, *121*, 159–175, doi:10.1002/2015JG003163.

Received 29 JUL 2015
Accepted 27 NOV 2015
Accepted article online 6 DEC 2015
Published online 16 JAN 2016

Evolution to decay of upwelling and associated biogeochemistry over the southeastern Arabian Sea shelf

G. V. M. Gupta[1], V. Sudheesh[1,2], K. V. Sudharma[1], N. Saravanane[1], V. Dhanya[1], K. R. Dhanya[1], G. Lakshmi[1], M. Sudhakar[1], and S. W. A. Naqvi[3]

[1]Centre for Marine Living Resources and Ecology, Ministry of Earth Sciences, Kochi, India, [2]Now at Department of Marine Biology, Microbiology and Biochemistry, School of Marine Sciences, Cochin University of Sciences and Technology, Kochi, India, [3]National Institute of Oceanography, Council of Scientific and Industrial Research, Dona Paula, India

Abstract Observations along 10 shelf transects in 2012 near 10°N in the southeastern Arabian Sea revealed the usual warm oligotrophic conditions during the winter monsoon and upwelling of oxygen-deficient, nutrient-rich cool water during the summer monsoon (SM). By changing an oligotrophic to a nutrient-replete condition, the upwelling is the major process that regulates the biogeochemistry of this shelf. Its onset is perceptible at 100 m depth between January and March. The upwelling reaches the surface layer in May and intensifies during June–July but withdraws completely and abruptly by October. Despite the nutrient injection, the primary production during SM, integrated for euphotic zone, is comparable to that during the preceding spring intermonsoon (SIM). Again, as usual, the high oxygen demand coupled with low concentration in the upwelled subsurface waters causes severe oxygen depletion below the shallow pycnocline. The oxygen concentrations/saturations of 2012 on the midshelf are similar from those of mid-1958 to early 1960, except for marginally higher values during the peak upwelling period due to relatively weak upwelling in 2012. This implies little anthropogenic influence on coastal hypoxia unlike many other coastal regions. In 2012, the inner shelf system shifted from net autotrophy in SIM to net heterotrophy in SM but on an annual basis it was net autotrophic (gross primary production to community respiration ratio, GPP/*R*:1.11 ± 0.84) as organic production exceeded consumption.

1. Introduction

This is the first published modern Kochi Time Series (KoTS) of nutrients and associated variables for the not well-studied upwelling off Kochi (Cochin; ~10°N), southwest India and is the second modern one for the west coast of India after Candolim Time Series (CaTS, since 1997) off Goa (15.5°N). Perennial upwelling is associated with the eastern boundary currents in the Pacific (Humboldt and California currents) and the Atlantic (Benguela and Canary currents). The surface currents flow toward the equator as part of the large-scale subtropical gyres as they do also during the summer monsoon (SM), but differs in the southeastern Arabian Sea (SEAS) in that it is not only driven by local winds but is also remotely forced [*Johannessen et al.,* 1987; *Shetye et al.,* 1990] and is quite rainy.

The seasonal reversal of winds and currents results in large changes in the mixed layer dynamics of the northern Indian Ocean, in particular, the Arabian Sea (AS), making it highly productive. During SM, both the western and eastern AS, especially the former, experience upwelling that brings cold, low oxygen and nutrient-rich waters to the surface. During winter monsoon (WM), convective mixing enhances nutrient levels in the euphotic zone leading to enhanced biological production in the northern AS [*Madhupratap et al.,* 1996; *Gardner et al.,* 1999; *Prasanna Kumar et al.,* 2001; *Wiggert et al.,* 2005]. The extensive oxygen minimum zone (OMZ; $O_2 < 20$ μM) in the open ocean is maintained by high O_2 demand for degradation of particles sinking from the surface layer and limited O_2 supply through horizontal advection. The OMZ in the AS is among the largest in the world, and its extension to the continental shelf during the upwelling period results in severe coastal hypoxia causing drastic changes in the biogeochemical properties including the emission of greenhouse gases [*Naqvi and Jayakumar*, 2000]. *Naqvi et al.* [2005] have identified the western continental shelf of India as one of the "hot spots" for oceanic N_2O emissions arising from seasonal anoxic/hypoxic events. The upwelling greatly influences the composition and abundance of marine life including fish eggs and larvae [*Bakun and Parrish*, 1982; *Balan*, 1984; *Johannessen et al.,* 1987; *Naqvi et al.,* 2006]. Hence, the

development of anoxia/hypoxia in shelf waters associated with upwelling is a major ecological event [*Naqvi and Jayakumar*, 2000; *Rabalais et al.,* 2001].

Time series observations are essential to understand seasonal and interannual variability of oceanographic processes and their response to human perturbations. Issues of particular concern are warming, eutrophication, deoxygenation, and acidification of seawater and their impacts on biogeochemical fluxes and ecosystem functioning. There is a dearth of long-term data from fixed sites in the Indian Ocean as compared to the Pacific and the Atlantic. However, the first time series study along the Indian coast was carried out by *Banse* [1959, 1968] off Kochi during 1958–1960. His study provided insight into the influence of SM on the hydrography and water composition of the SEAS. Banse opined that upwelling and sinking were mainly caused by the currents and not the winds, as reported earlier by *Rama Sastry and Myrland* [1959]. *Banse* [1959] also reported 4–5°C variation in sea surface temperature with annual maximum during April–May and minimum in July–August based on 16 years of surface data in the sea off Calicut (~11.3°N, SEAS). Subsequent studies aimed at explaining the physical dynamics of upwelling [*Sharma*, 1978; *Johannessen et al.,* 1987; *Schott and McCreary*, 2001; *Shankar et al.,* 2002; *Shenoi et al.,* 2005; *Jayaram et al.,* 2010], but its biogeochemical effects were not studied in detail. Subsequently, the two other time series measurements being made off Goa since 1997 (Candolim Time Series, CaTS) in the AS [*Maya et al.,* 2011] and off Visakhapatnam (since 2007) in the Bay of Bengal [*Sarma et al.,* 2013] revealed regional variability of the response of tropical seas to long-term changes in the climate. As the SEAS experiences conditions that are different from these shallow time series sites, sustained observations were initiated off Kochi and named as Kochi Time Series (KoTS). The data collected in 2012 are used here to address (i) seasonal evolution and termination of upwelling process, (ii) distribution of nutrients in response to the changing physical and biogeochemical processes, (iii) comparison of O_2 saturations with historical data, and (iv) net ecosystem metabolism.

2. Study Area

The biogeochemistry of the SEAS is closely linked to the seasonally changing coastal currents by northward and southward flowing West India Coastal Current (WICC) during WM and SM, respectively. The transition seasons viz., spring intermonsoon (SIM) and fall intermonsoon (FIM) exhibit mixed signals between SM and WM. The northerly current during WM carries low-salinity water originating in the Bay of Bengal fortifying stratification in the upper water column. During SM the upwelling-induced nutrient enrichment leads to high biological production over the western continental shelf of India. One of the important aspects of the SEAS is the seasonal hypoxia/anoxia arising from increased oxygen demand for mineralization of organic matter following high surface production. Many small rivers like the Mandovi and Zuari in Goa, the Kali in north Kanara, and the Netravati in south Kanara flow across the coastal plain and discharge into the AS. The Cochin backwaters (CBW), the largest estuarine system of the southwest coast of India, is connected to the SEAS. CBW receives 1.04×10^5 m^3 of industrial and 260 m^3 of domestic wastes per day without treatment [*Balachandran et al.,* 2005] and is highly heterotrophic in nature [*Thottathil et al.,* 2008; *Gupta et al.,* 2009]. This is expected to influence the biogeochemistry of the adjoining sea considerably.

3. Materials and Methods

Time series sampling was carried out along a transect of the shelf off Kochi (KoTS, Figure 1) 10 times from January to December 2012 (approximately 30–45 days interval) on board Fishery Oceanographic Research Vessel (FORV) *Sagar Sampada*. Six stations (bottom depth 13, 20, 30, 40, 50, and 100 m) were occupied for collections from standard depths (surface, 10, 20, 30, 40, 50, 75 and 100 m). On most occasions, sampling began in the morning (station 1) and was completed in the evening (station 6). The details of sampling dates and phase of the tide are given in Table 1. Station 1 is located in the dredged navigation channel for the Cochin port which connects the estuary and the sea. For convenience, the continental shelf is classified into four regions with station 1 being nearshore, stations 2 and 3 over inner shelf, stations 4 and 5 over midshelf, and station 6 representing the outer shelf.

Temperature and salinity profiles were recorded using a conductivity-temperature-depth (CTD) profiler (SBE 11 Plus, Sea-Bird, Redmond, WA, USA). Water was collected using Niskin samplers (5 L) mounted on the CTD rosette. Samples for dissolved oxygen (O_2) were collected in 60 ml glass bottles, fixed with 0.5 ml

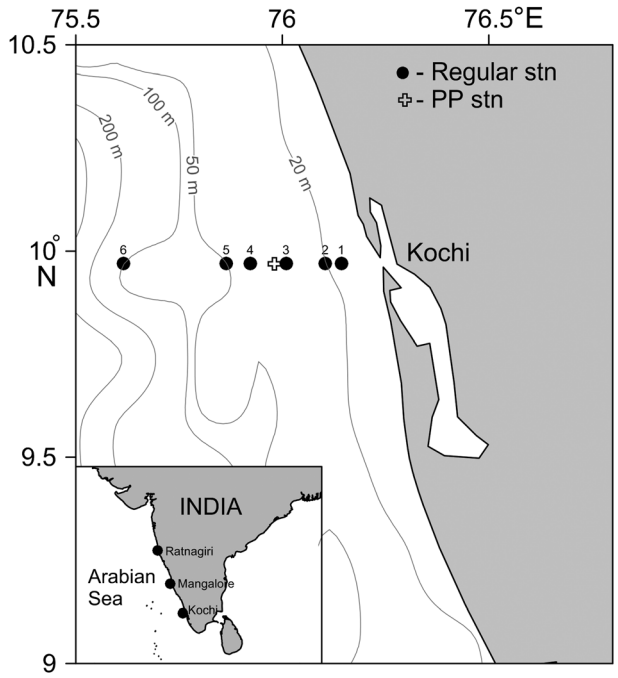

Figure 1. Location map for Kochi time series (KoTS) of 2012 in the southeastern Arabian Sea.

each of Winkler reagents and titrated onboard against 0.001 N thiosulphate with starch-based visual end point detection [*Grasshoff et al.,* 1999]. Assuming that NO_2^- levels would be generally low, sodium azide was not added for preventing interference with O_2 [*Wong*, 2012]. The small amount of O_2 carried by the reagents was not considered. The detection limit was about 2 μM. O_2 saturation was computed following *Garcia and Gordon* [1992]. Samples for nutrients (nitrate, nitrite, ammonium, phosphate, and silicate) were analyzed colorimetrically (Evolution 201, Thermo, USA) within a few hours of collection on board the ship following standard procedures [*Grasshoff et al.,* 1999]. The analytical precision expressed as standard deviation for nitrate, nitrite, ammonium, phosphate, and silicate were ±0.05, ±0.01, ±0.07, ±0.02, and ±0.03 μM, respectively. Samples (2 L) for chlorophyll *a* (Chl *a*) estimation were filtered onboard through Whatman 47 mm GF/F filter (0.7 μm) under gentle vacuum (<50 mm Hg) and kept at −20°C till the analysis. Chl *a* in the filters were extracted with 90% acetone at 4°C in the dark for 12 h and measured fluorometrically [*Joint Global Ocean Flux Study*, 1994]. Biovolume of surface mesozooplankton in samples collected using Bongo net (300 μm) was estimated on board by the displacement method after removing surplus water by absorbent paper.

Gross primary production (GPP) and community respiration (*R*) were measured in situ by the O_2 method with light and dark bottles (LB and DB, respectively) collected from and incubated at the surface, 10, 20, and 30 m at a station located ~25 km away from the shore (close to station 3), where depth is ~33 m, referred to as the PP station. These incubations were done on the day following regular section work. However, nutrients and Chl *a* data collected at station 3 on the preceding day of incubation have been used to explain the variations in metabolic rates assuming insignificant variation between successive days. Water samples were collected in two sets (as LB and DB) of three BOD (biological oxygen demand) glass bottles (300 ml); each were attached to a polypropylene rope and incubated in situ for 24 h (0600 to 0600 h). The dark bottles were wrapped with aluminum foil and black tape. The O_2 was analyzed immediately after retrieval on board the ship. The net community production (NCP), community respiration (*R*), and gross primary production (GPP) were calculated from O_2 changes (with "*I*" denoting initial O_2), by LB − *I*, *I* − DB, and NCP + *R*, respectively. The metabolic rates measured as O_2 were converted to carbon equivalents assuming a photosynthetic quotient of 1.2 and respiratory quotient of 1 [*Laws*, 1991]. Net primary production (NPP) in the same samples was also measured in situ as ^{14}C uptake [*Joint Global Ocean Flux Study*, 1994]. Paired LB and DB Nalgene polycarbonate

Table 1. Sampling Inventory Details With Phase of the Tide

Survey Number	Sampling Period (2012)		Station 1	
	Month	Dates[a]	Starting Time (h)	Phase of the Tide
1	January	21–23	1400	Low Tide
2	March	3–5	0620	Intermediate
3	April	13–15	0600	Intermediate
4	May	23–25	0500	Low Tide
5	June	28–30	0615	High Tide
6	July	27–29	0600	High Tide
7	September	1–3	0900	Intermediate
8	October	5–7	0950	Low Tide
9	November	9–11	0620	High Tide
10	December	8–10	0510	High Tide

[a]Transect sampling made on the first day and PP incubation on subsequent day.

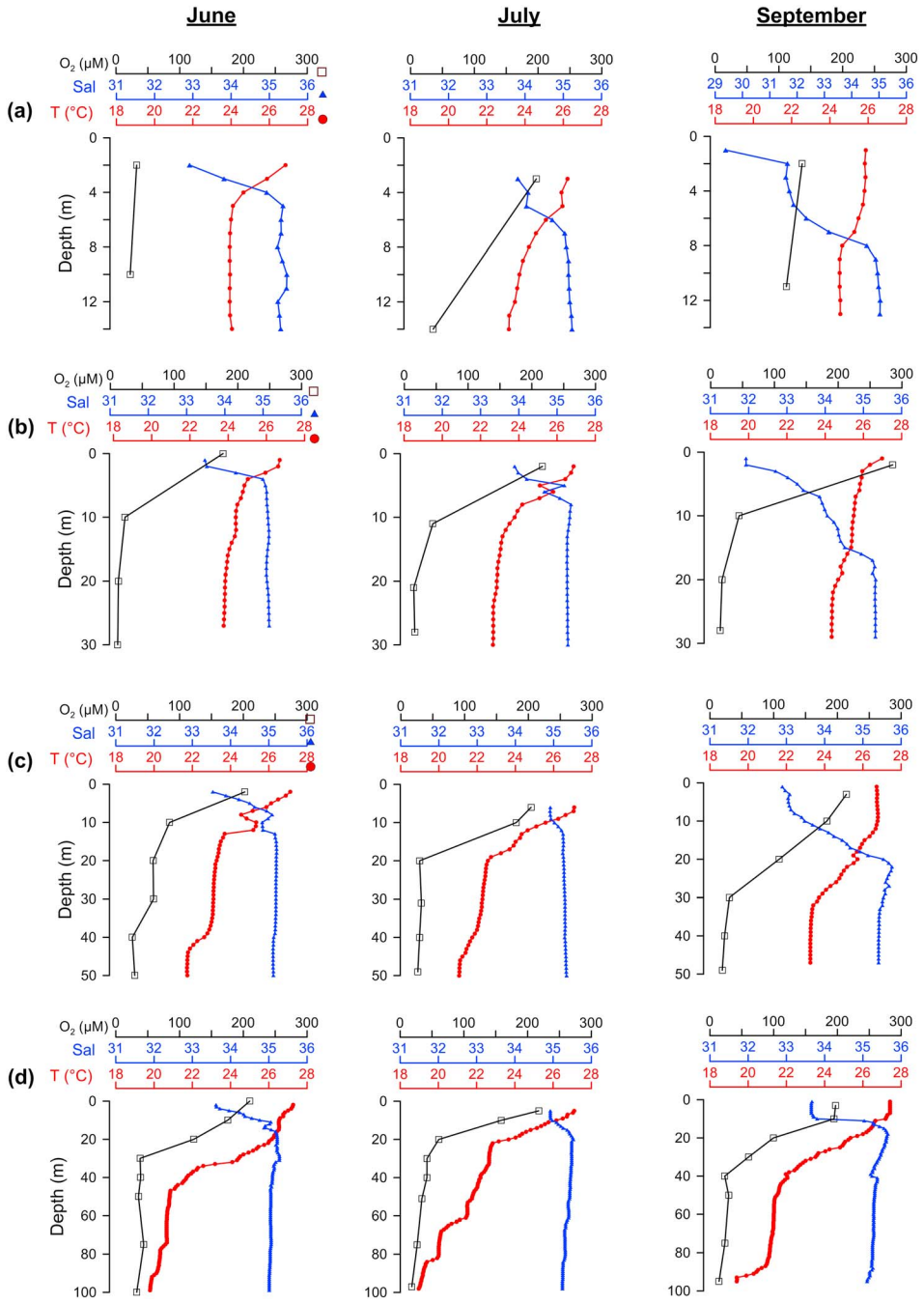

Figure 2. Vertical profiles of temperature, salinity and dissolved oxygen at (a) station 1 (nearshore), (b) station 3 (inner shelf), (c) station 5 (midshelf), and (d) station 6 (outer shelf) during summer monsoon months.

bottles with 250 ml sample each were inoculated with $NaH^{14}CO_3$ (activity 5 μCi ml^{-1}, Bhabha Atomic Research Centre, India; with 1 ml of this strength per bottle) and incubated along with BOD bottles for 12 h during daytime. On retrieval, water samples were immediately passed through Whatman 25 mm GF/F filter (0.7 μm) under gentle vacuum (<50 mm Hg) in diffused light and kept at −20°C until analysis. The excess labeled dissolved inorganic carbon on the filter was removed by exposing them to fumes of concentrated hydrochloric acid for 1 min. The filters were then placed in scintillation vials with 5 ml cocktail (dioxane). Radioactivity was measured by a liquid scintillation counter (Beckman Coulter LS6500). NPP rates were calculated based on a 12 h photo period and expressed as mg C m^{-3} d^{-1}. A Secchi disc was used to estimate the

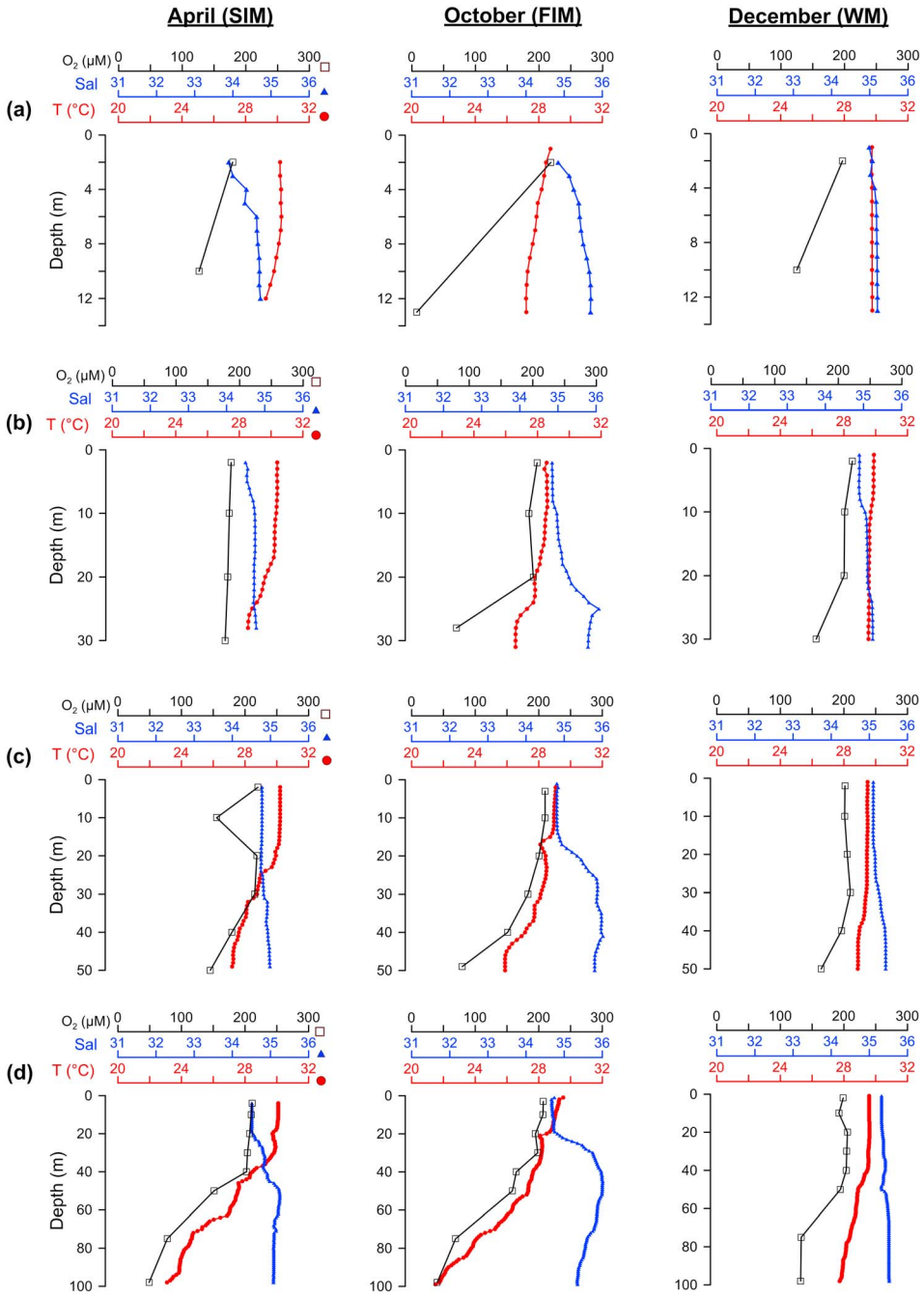

Figure 3. Vertical profiles of temperature, salinity and dissolved oxygen at (a) station 1 (nearshore), (b) station 3 (inner shelf), (c) station 5 (midshelf), and (d) station 6 (outer shelf) during months other than summer monsoon.

euphotic depth (2.8 × Secchi depth) [*Richard et al.*, 1982] which was rounded off to the nearest sampling depth to calculate photic column integrated metabolic rates.

4. Results

4.1. Hydrography

The sea surface temperature (SST) exhibited a progressive warming between January (>28°C) and April (>30°C) during spring intermonsoon (SIM, March−April). By May, the waters over the inner shelf began to cool and cold waters persisted through the summer monsoon (SM, June–September). The mixed layer depth (MLD; 0.2 density

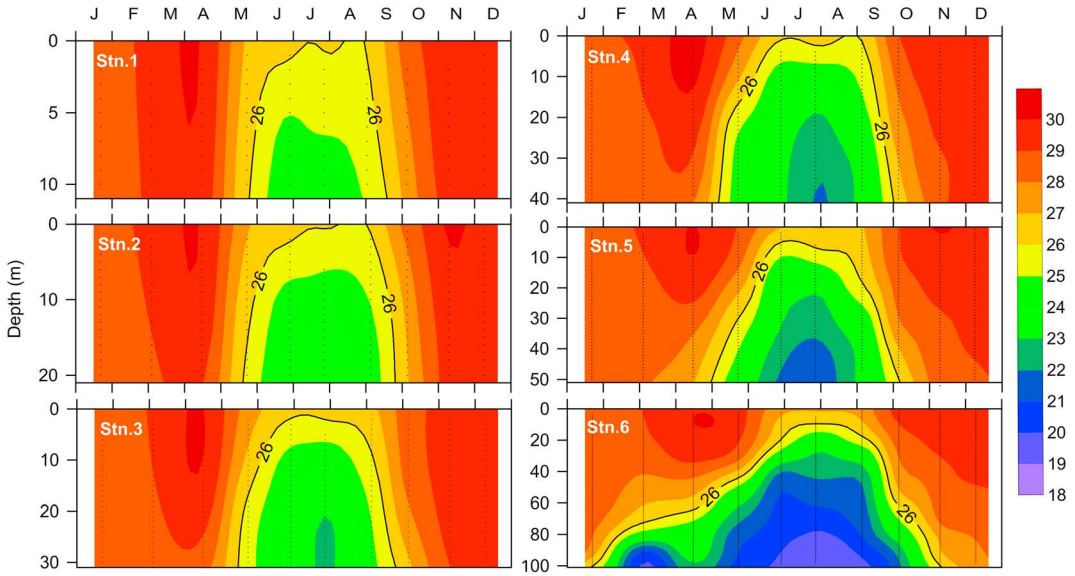

Figure 4. KoTS monthly variation in temperature (°C) for all stations.

difference from surface) was thin (up to 20 m) during SM (Figure 2) and deepened (up to 50 m) during winter monsoon (WM, November–December, Figure 3). The depth of the 26°C isotherm (D_{26}) generally followed closely with MLD (Figure 4). Therefore, D_{26} is utilized here to describe the progression of upwelling. D_{26} was located at 100 m over the outer shelf during January, but it shoaled progressively to 80 m by March, remained invariable up to April but shoaled up to 10 m by July. Thereafter, it showed downward movement to 20 m by September and then it sharply deepened to ~70 m by October before its complete disappearance in November. The observations reveal the following: (i) initiation of upwelling in the deeper layers during January–March and its progression to the upper layers during June–September, (ii) sharp withdrawal of upwelling during October–November. While the intensification of upwelling took about 4 months from April to July, its collapse happened within a month. The D_{26} appeared over the midshelf only by the end of April and over the inner shelf by the middle of May indicating that the advancement of upwelling between outer and midshelf took longer time (100 days at 0.22 km d^{-1}) than from middle to inner shelf (15 days at 1.29 km d^{-1}). The rate of upwelling in terms of vertical upliftment of isotherms is on the order of 1.3–1.9 m d^{-1}. This is in agreement with ~1.5 m d^{-1} reported earlier for the SEAS by *Johannessen et al.* [1987]. The upwelling is generally slow to begin with (March–April), but it gets momentum by May as D_{26} shoaled from about 45 m to 15 m and extended ~30 km toward the coast. By July, the D_{26} has reached the surface close to the coast indicating the complete and peak spreading of upwelling to the entire shelf region, which sustained up to August. Similarly, the withdrawal of upwelling followed a sequence with the sharp withdrawal of D_{26} from the nearshore region to midshelf during August–September and finally from the outer shelf by end of October. Consequently, SST increased by 2–3°C during November–December.

During WM and the beginning of SIM, the surface waters over the shelf off the southwest coast of India are advected from the Bay of Bengal [*Prasanna Kumar et al.,* 2001] which are warm (>28°C) and relatively fresh (salinity < 34.5). Parallelly, the outer shelf experienced the intrusion of Arabian Sea High-Salinity Water (ASHSW) at depth through upwelling resulting in stratification of the water column (Figures 3 and 5). In April the ASHSW waters advanced into the midshelf through upwelling, and the Bay of Bengal Low-Salinity Water (BBLSW) had completely withdrawn from the outer shelf and even started withdrawing from the middle and inner shelves. This indicates that the displacement of BBLSW from the SEAS under the advent of upwelling progresses from the outer shelf to the inner shelf. A clear uplift of 35.5 isohaline from ~80 to 60 m (March–April) and further to ~15 m in May is due to the penetration of ASHSW into the shelf region through upwelling.

The monsoon precipitation considerably lowered the surface salinity to <34 (June–September) and established strong stratification. According to *India Meteorological Department* [2013], 2012 was an Indian Ocean Dipole (IOD) year with a relatively short duration during July–October; the IOD index was near neutral during June–July and positive from the beginning of August that resulted in deficient monsoon rainfall over the

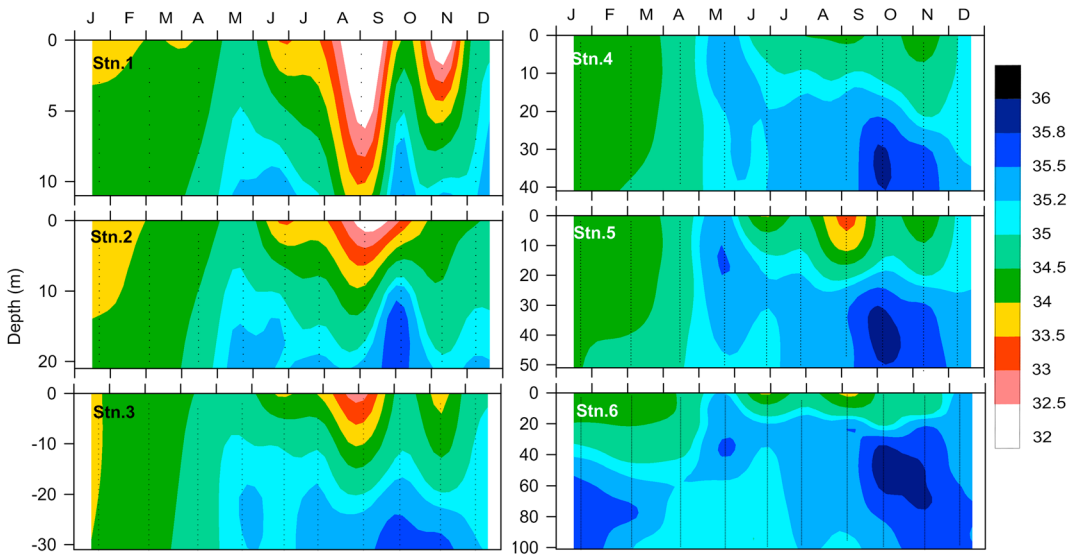

Figure 5. KoTS monthly variation in salinity for all stations.

Indian subcontinent during the first half of the season followed by neutral and above normal rainfall during August and September, respectively. Consistent to this, the study region did receive considerable rainfall just before our June and September observations, but the period preceding the July observations was largely dry when the upwelling was at peak. This pattern of rainfall is clearly reflected in the surface salinity distribution during SM (Figures 2 and 5) with the lowest recorded in September.

4.2. Monthly Variations in O_2, Nutrients, and Chl *a*

The distribution of O_2 (Figures 2 and 3 and Figure S1 in the supporting information) and nutrients (Figures 6, 7, and S2–S6) showed marked seasonal variations. The high O_2 (>200 μM) and low nutrients (NO_3: <0.5 μM; PO_4: 0.2–0.3 μM) in the upper 50 m in January indicate well-oxygenated, oligotrophic condition as stratification limits upward flux of nutrients. Although the conditions in the euphotic column showed little change up to April, upwelling brought low-O_2 (~70–80 μM) and high-nutrient waters at depth over the outer shelf. The low-O_2 and high-nutrient water continued to advect toward the inner shelf and spread over the entire shelf region by September. The maximum effect of upwelling was seen between May and June which turned the subsurface waters (>30 m) hypoxic (<50 μM) and nitrate rich (>10 μM). Ammonium concentrations were <0.5 μM at all depths between the outer and midshelf regions (Figure S4). Similar to N and P, silicate concentration also showed enrichment during SM upwelling (Figure S6). These seasonal sequences of subsurface changes in hydrography, O_2, and nutrients of 2012 are similar to the results by *Banse* [1968], *Rao and Ramamirtham* [1976], *Sharma* [1978], *Menon and George* [1977], and *Johannessen et al.* [1987]. The impact of upwelling was severe in surface waters of coastal stations (stations 1 and 2) in June, where the O_2 saturation was at its minimum (6.75% and 15.6%, respectively) and nutrient levels were at their maxima. These stations are affected by the monsoon discharges from the Cochin estuary, but as the sampling was conducted during the high tide in June (Table 1), the influence of runoff in the nearshore region is not expected to be very high. The atmospheric fallout of N through rainfall (~4 μM of nitrate) [*Naqvi et al.,* 2000] also adds to the mixed layer concentrations, but this is much smaller relative to the supply through upwelling. High concentrations of nitrite in the nearshore and inner shelf regions in June (up to 3.2 μM, Figure 6) are associated with a corresponding increase in N_2O (164 nM, Sudheesh et al., in preparation, 2015). The minimum O_2 concentration of 7 μM (Figure 2) is expected to inhibit denitrification in the water column, but it is most likely that denitrification occurred in the anoxic seabed. Primary nitrite maximum was seen mostly at the bottom of euphotic zone, for example, at station 3 intermediate depths during SM (Figure 6) and close to the bottom during nonupwelling periods (Figure 7) due to oxidation of excretes of secondary producers and nitrification of ammonia. Similar maximum was also observed over the midshelf off Kochi during 1958–1960 (K. Banse, personal communication, 2014). The transition in October was distinguished by a sharp decline in nutrient

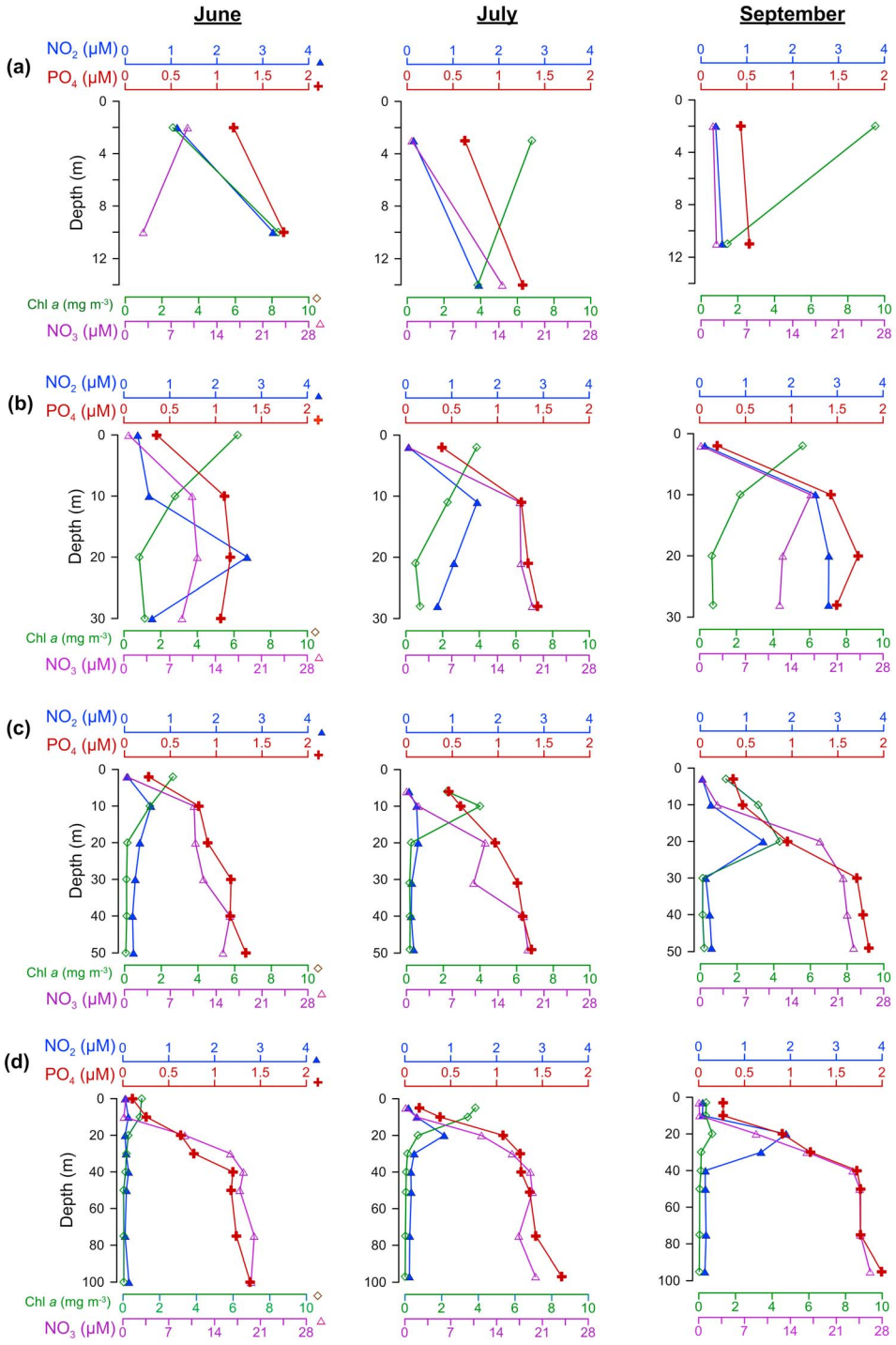

Figure 6. Vertical profiles of nutrients and chlorophyll *a* at (a) station 1 (nearshore), (b) station 3 (inner shelf), (c) station 5 (midshelf), and (d) station 6 (outer shelf) during summer monsoon months.

concentrations (NO_3: 0.49 ± 0.5 μM, NO_2: 0.16 ± 0.2 μM; PO_4: 0.29 ± 0.1 μM; Figure 7) and rise in O_2 level (>150 μM; Figure 3) following the abrupt withdrawal of upwelling. Subsequently, the MLD deepened and the O_2 concentrations increased further to ~200 μM.

The nutrient ratios especially Si/P (9.2 and 8.0) and Si/N (0.54 and 0.68) remained almost similar between summer upwelling (June–September) and the rest of the year (Figure 8), but the N/P ratio was high and close

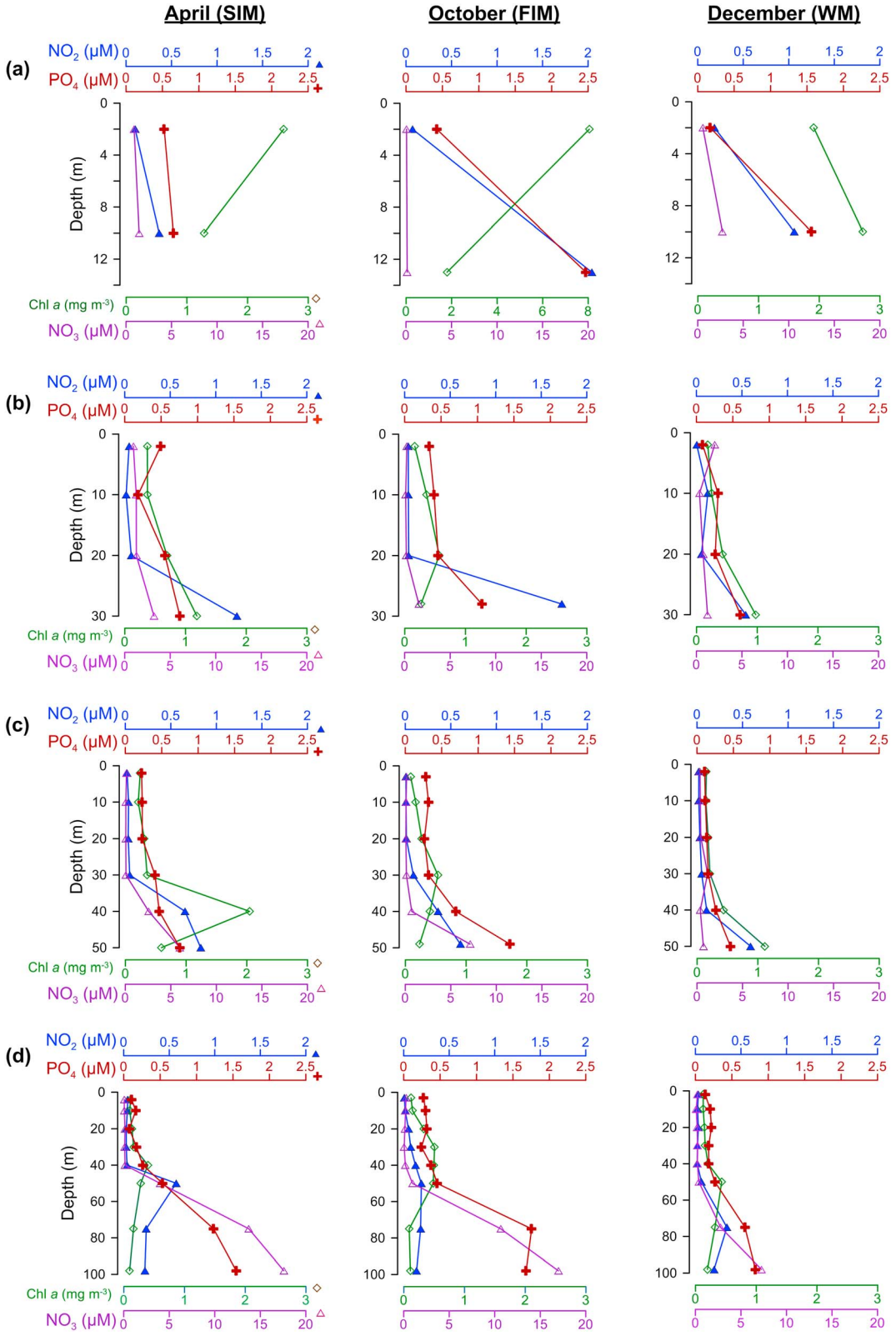

Figure 7. Vertical profiles of nutrients and chlorophyll *a* at (a) station 1 (nearshore), (b) station 3 (inner shelf), (c) station 5 (midshelf), and (d) station 6 (outer shelf) during months other than summer monsoon.

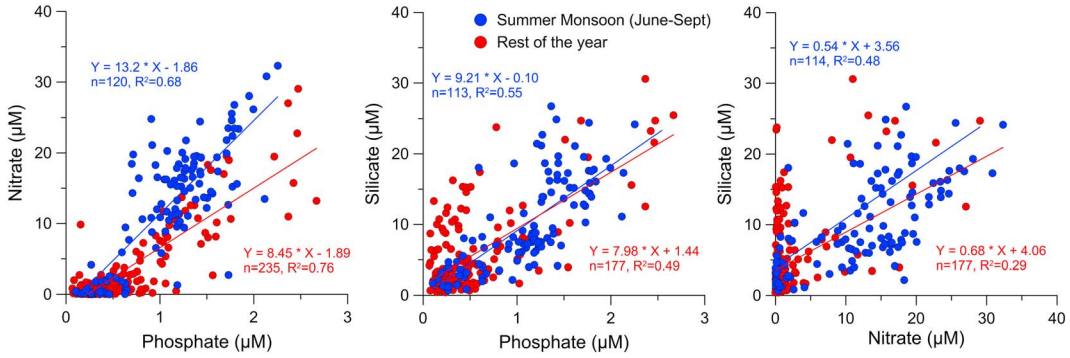

Figure 8. Variation in stoichiometric ratios of nutrients between summer monsoon and the rest of the year.

to the Redfield value during upwelling (13.6) compared to nonupwelling period (8.8) suggesting nitrogen deficiency during the latter period. Among the nonupwelling seasons, the N/P ratios during SIM (9.7) and WM (9.6) were practically undistinguishable and higher than those during FIM (7.3).

The Chl *a* concentration was low during January–March (0.01–0.62 mg m^{-3}; Figure S7) but increased in April due to the proliferation of *Trichodesmium erythreaum* [*Jabir et al.,* 2013] under the prevailing calm, warm, and bright sunlight conditions. Subsurface chlorophyll maximum (SCM) was continually seen during this period (Figure 7) supported by deeper photic depths and nutrients injection (at the outer shelf) following upwelling. During this period, Chl *a* increased to 2.59 mg m^{-3} in nearshore waters along with nutrients (NO_3: 0.83 μM and PO_4: 0.52 μM). Apart from the intraannual variation, the recent satellite-based studies of *Jayaram et al.* [2010]

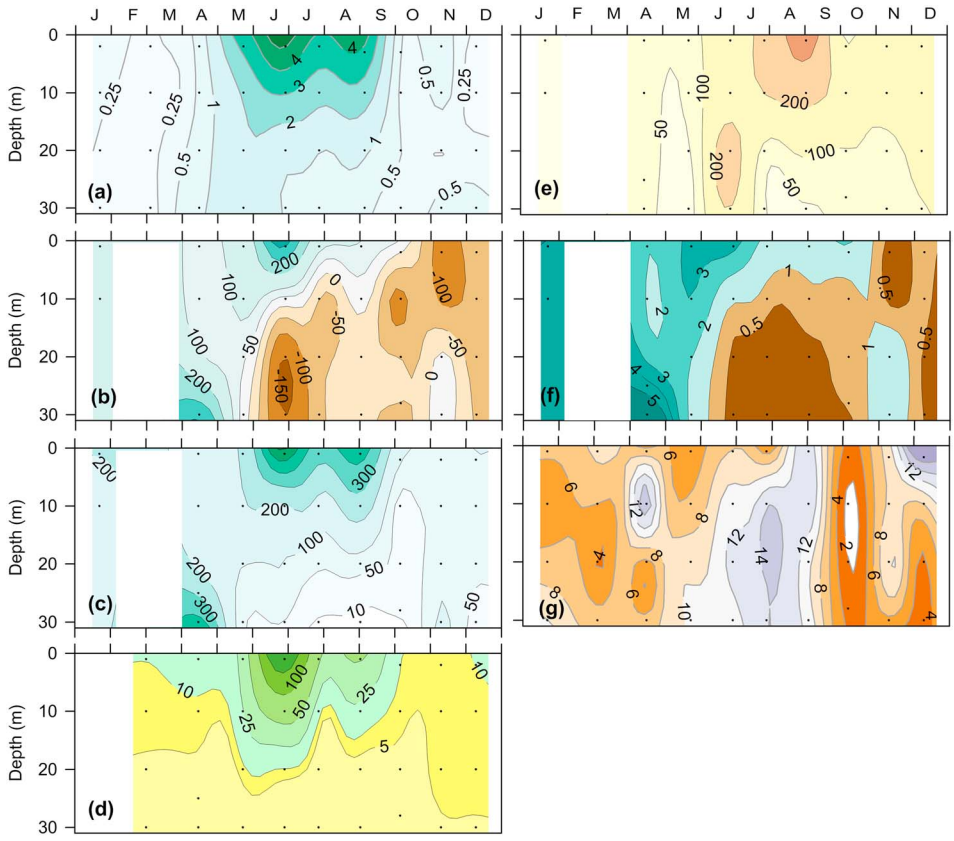

Figure 9. Time series changes in metabolic rates (a) Chl*a* (mg m^{-3}), (b) NCP, (c) GPP, (d) NPP, (e) Community Respiration, (f) trophic status represented by GPP/R ratio, and associated changes like (g) N/P ratio at PP station (refer Figure 1). All metabolic rates are expressed in mg C m^{-3} d^{-1}.

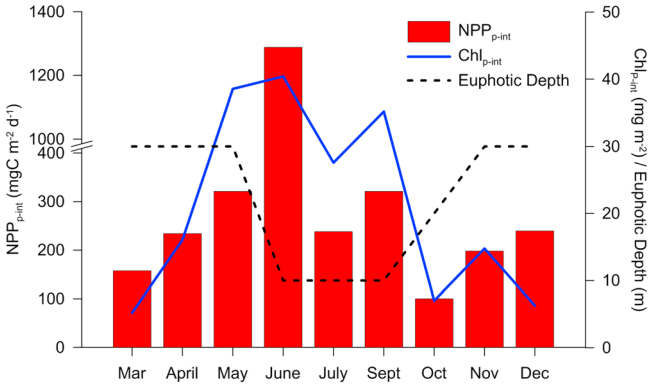

Figure 10. Monthly changes in euphotic depth, photic column integrated NPP, and Chl*a* at PP station.

and *Shalin and Sanilkumar* [2014] also reported significant interannual variation in Chl *a* concentrations in the SEAS chiefly due to variation in upwelling intensity. With the onset of SM, since nutrients were adequately available, the SCM disappeared, especially over the inner shelf, as the enhanced phytoplankton production is limited mostly within the shallow photic depth (~10 m; Figure 6) due to the monsoon cloud cover. High Chl *a* levels were observed in the upper 20 m beyond the inner shelf during July when the region experienced completely dry conditions (at least for 10 days) prior to the sampling period with no cloud cover resulting in deeper euphotic zone as compared to June. Thus, the availability of nutrients and sunlight promoted phytoplankton growth within the euphotic column in July. The withdrawal of SM in October quickly reduced the chlorophyll levels to the pre-SM levels culminating in oligotrophic conditions by December (Figure 7). The environmental conditions during WM were almost similar to those during SIM, and the deeper photic depths favored reappearance of SCM, albeit with low magnitude that the oligotrophic condition supported proliferation of relatively less intense *Trichodesmium* blooms in November–December.

4.3. Plankton Metabolic Rates

The plankton production and respiration rates along with N/P ratios at the PP station are shown in Figure 9. The net community production (NCP) was positive between January and May, but from June through October the NCP was negative between 10 and 30 m depths. In November, the NCP was negative up to 10 m and positive below this depth, but in December, the NCP was negative in the entire water column. The Chl *a* maximum at the bottom, in April, was responsible for the high NCP and GPP rates but did not affect the NPP. The NPP rates during SIM were more than double of that during WM, whereas it was the other way around for respiration (*R*) rate, which was the highest in the upper 10 m during July–September. The NCP, GPP, and NPP rates in the photic zone (within the upper 10 m) during SM responded positively to the increase in Chl *a* and exhibited similar maxima. The respiration rate in the surface layers also showed a twofold to threefold rise during SM though it was lower than the GPP. The respiration rate during October–December was almost twice that of pre-SM rates.

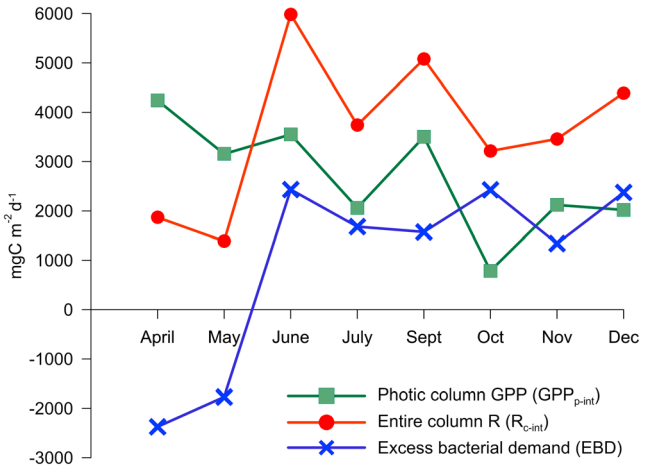

Figure 11. Monthly changes in column integrated GPP, R, and EBD rates at PP station.

The photic column integrated Chl *a*, GPP, and NPP, represented as Chl$_{p\text{-}int}$, GPP$_{p\text{-}int}$, and NPP$_{p\text{-}int}$, respectively, and the column-integrated *R*, represented as $R_{c\text{-}int}$, are presented in Figures 10 and 11. NPP$_{p\text{-}int}$ increased progressively from March to May before peaking in June following upwelling and increase in Chl$_{p\text{-}int}$. The NPP$_{p\text{-}int}$ during WM was comparable to that in April and July, but the corresponding Chl$_{p\text{-}int}$ showed significant variation. Similar to NPP$_{p\text{-}int}$, GPP$_{p\text{-}int}$ in WM was almost comparable with that during July, whereas the $R_{c\text{-}int}$ during the former period was higher than that during the latter period. NPP$_{p\text{-}int}$ was at its minimum in

October (100 mg C m^{-2} d^{-1}) coinciding with the GPP_{p-int} minimum (780 mg C m^{-2} d^{-1}) following the cessation of upwelling, whereas the maxima in these properties did not coincide with the former occurring in June (1290 mg C m^{-2} d^{-1}) and the latter in April (4240 mg C m^{-2} d^{-1}). The highest $R_{c\text{-}int}$ was recorded in June coinciding with the highest $NPP_{p\text{-}int}$ and $GPP_{p\text{-}int}$.

5. Discussion

The upwelling along the west coast of India is forced not only by local winds but also by Kelvin waves originating in the Bay of Bengal and traveling around Sri Lanka [*McCreary et al.,* 1993; *Shankar and Shetye*, 1997], but the exact forcing mechanism for its early occurrence (January–March) is still unknown. The northerly flowing WICC favors the formation of anticyclonic gyre in the Lakshadweep Sea during January causing sinking of surface waters, leading to the formation of Lakshadweep high [*Bruce et al.,* 1994; *Shankar and Shetye*, 1997; *Shenoi et al.,* 1999]. This influence the shelf surface waters to move offshore, the mass transported will be balanced by the rising of subsurface waters, initiating upwelling at depth. Although the Modular Ocean Model output showed northerly currents in the SEAS during January–April 2012 for a very short period between 28 February and 14 March 2012, the currents distinctly reversed from northerly to southerly (M. Ravichandran, personal communication, 2014). The model results (2004–2012) also showed that such anomalous reversal of coastal currents for a brief period recurs every year during January–April. Although Sea Surface Height Anomaly (SSHA) increased (>6 cm) during January–April, there was a short period during the first half of March when the SSHA dropped abruptly by 6–8 cm (see Figure S8) probably in response to the anomalous reversal of coastal currents. Although the exact cause of this brief anomalous feature is unknown, this period was also characterized by the advection of offshore waters at depth (outer shelf), perhaps as a consequence of the initiation of upwelling by the reversal of currents.

5.1. Comparison With Historical Data (1958–1960)

Banse [1968] carried out the first time series measurements of hydrographical parameters in Kochi coastal waters (50 m, ~45 km away from the coast) from July 1958 to January 1960. We compare his results with the present time series from the same location (station 5; Figure 12) especially in contradiction with any change in O_2 saturation. As stated earlier, 2012 was an IOD year and registered positive SST anomalies in the western Indian Ocean. The year 1958 was a negative IOD year whereas 1959 was a normal year (http://www.marine.csiro.au/~mcintosh/Research_ENSO_IOD_years.htm). The 1958–1959 data had shown strong interannual variability with a shift in the peak upwelling from August to October (in 1958 after ~1.5 months without data) in successive years whereas the 2012 data exhibited peak upwelling in July. D_{26} was completely displaced from the water column by cold water during peak upwelling in 1958, whereas it reached the surface during the corresponding period in 1959 and about 10 m in 2012 (Figure 13). Similarly, the bottom was penetrated by the 20°, 21°, and 22°C isotherms during peak upwelling in 1958, 1959, and 2012, respectively. This suggests that upwelling during 2012 was relatively weaker than in 1958 and 1959. Based on depth change in D_{26}, the progression of upwelling has been found to be relatively faster in 2012 (2 months, May–July), whereas it lasted much longer in 1959 (June to October). However, the withdrawal of upwelling took about 2 months in 2012 which is comparable with that in 1958 but took less than a month in 1959. Salinity showed marked variations between the two sets of observations; especially at the surface, it was lower by more than one unit during WM and SM of the former period. High salinity of 35.2–35.5, a signature of ASHSW, was mostly seen in the subsurface layers in 2012; such water mass was observed only during 1959 but not in 1958.

The O_2 saturation was generally similar among the years (Figure 12). However, a close look during peak upwelling periods (Figure 13) revealed that the upper 10 m O_2 saturations increased from ~18% in 1958 to ~50% in 1959 and 86% in 2012, but below this depth saturation levels are only marginally higher (6–10%) in 2012 as compared to earlier years. This can be due to (i) increased anthropogenic effects, (ii) variation in upwelling intensity or source water characteristics, and (iii) both. A recent study [*Martin et al.,* 2010] revealed a sixfold increase in nitrate and phosphate concentrations and fourfold increase in sediment organic carbon in the lower reaches of the adjoining Cochin estuary (CE) between 1965 and 2005 due to large-scale developmental activities. Our parallel study in the CE shows that the turnover time of dissolved inorganic nitrogen (DIN) pool was very fast (11 ± 7.6 h for NH_4 and 118 ± 115 h for NO_3 during September 2012) as the substrate renewal rates largely sustained high N uptake reflecting the estuarine response to increased human impacts

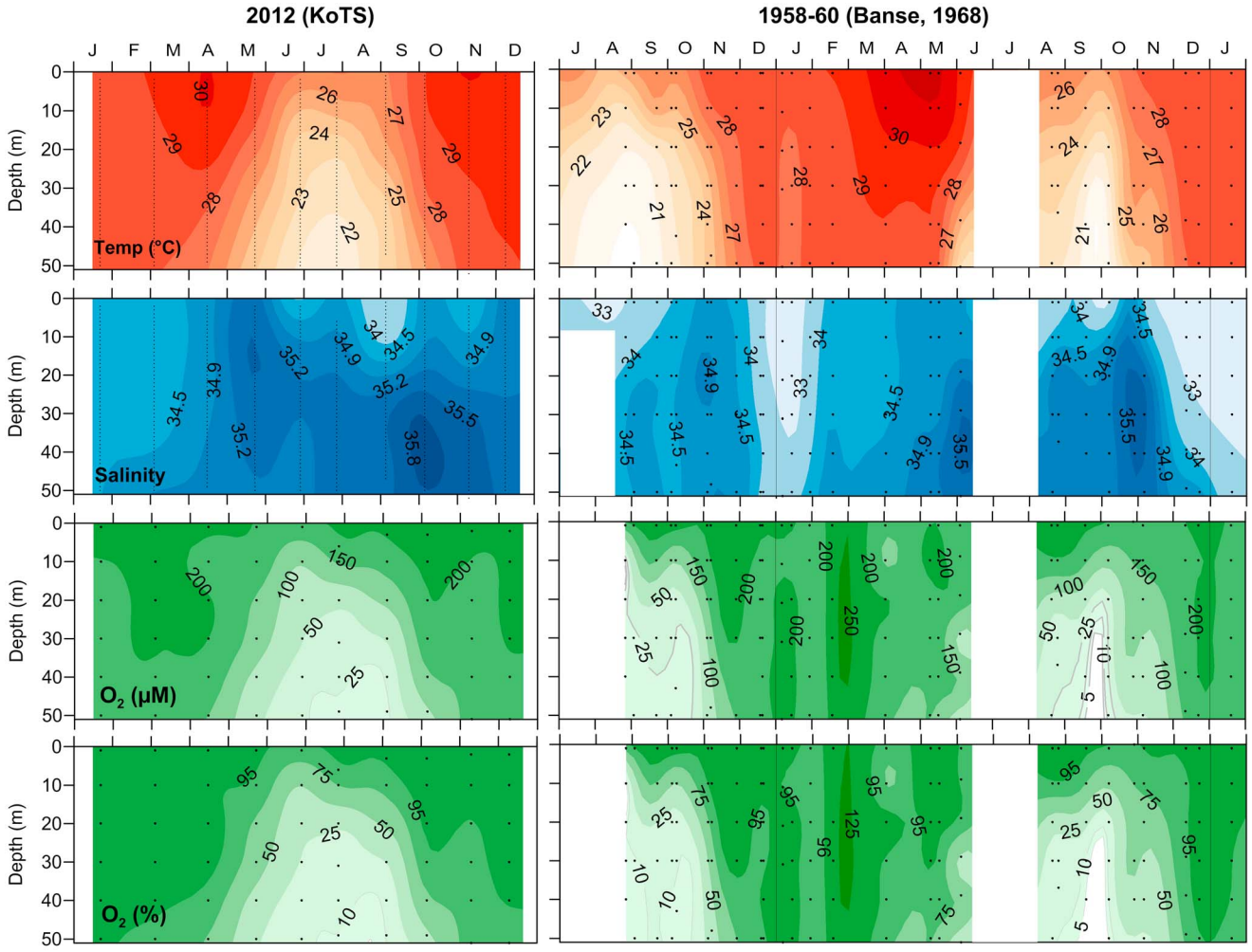

Figure 12. Comparison of KoTS 2012 results at station 5 with those of 1958–1960 [*Banse*, 1968, Figure 2] off Kochi. The replotted data, published by *Central Marine Fisheries Research Institute* [1964] and in principle also available from data centers, were kindly provided by K. Banse, Oceanography, University of Washington, Seattle, WA, USA. Reproduced with permission from the publisher.

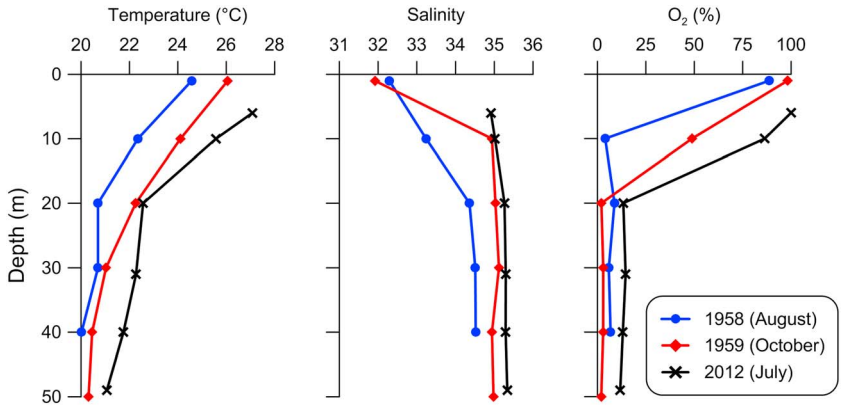

Figure 13. Comparison of historical profiles corresponding to peak upwelling months (refer to Figure 12).

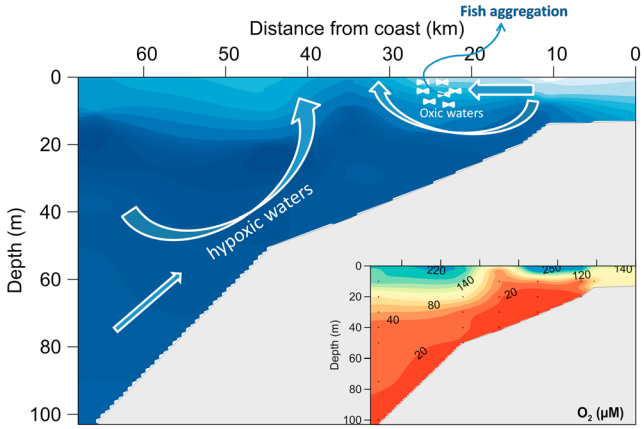

Figure 14. Schematic picture showing the fish aggregation on the inner shelf during an episodic event in September 2012. The background blue contours represent the salinity distribution; i.e., intensity of blue color increases with increasing salinity. The arrows represent the movement of two water masses in opposite direction. The inset picture shows the corresponding dissolved O_2 concentration.

[*Bhavya et al.,* 2015]. The flushing time of estuary during monsoon (~5 days based on *Gupta et al.* [2009]) supports the argument that much of the anthropogenic DIN is utilized within the estuary. This is in agreement with the studies from the Godavari estuary on the east coast of India [*Sarma et al.,* 2009, 2010]. Despite this, the CE still exports significant fraction of DIN to the coastal sea during SM (for example, 5.5 μM of NH_4^+ and 12.9 μM of NO_3^- at the surface of CE mouth with salinity 5.36 during September 2012) causing O_2 depletion. However, this is largely found to extend only up to station 3 (see Figures 2, 5, 6, and S1–S6). Therefore, the observed variations in O_2 saturations at station 5 can be attributed largely to the upwelling source water characteristics (nutrients, oxygen, etc.).

Understandably, coastal hypoxia during upwelling is dynamically linked to the offshore oxygen minimum zone (OMZ). Upwelling supports moderately high primary production which in turn causes further depletion of oxygen from an already oxygen-deficient waters that upwell over the shelf. Coastal waters off Kochi have never been found to be fully anoxic (sulphidic) in the last four decades, but such conditions recur every year north of Mangalore (12.8°N) [*Naqvi et al.,* 2009]. We could also identify an anoxic layer off Mangalore (unpublished data) and a suboxic condition (8–10 μM O_2) off Kochi during September 2012 (Figure 2). This is because the upwelling source (offshore) water at Mangalore is relatively cold, less saline, and more oxygen depleted as compared to warmer, saltier, and less oxygen-depleted water off Kochi. The O_2 within the OMZ decreases northward, including in the West India Undercurrent that is a source of water upwelling over the shelf [*Naqvi et al.,* 2006]. Moreover, the northern Arabian Sea processes (especially the winter convective mixing which has large interannual variability) largely influence the upwelling source waters north of Mangalore but not off Kochi. As discussed earlier, stronger upwelling off Kochi brought up the poorly ventilated waters to shallower depth (10 m) in 1958–1959 compared to 2012 (20 m) which resulted in the greatest difference in O_2 saturations at 10 m (Figure 13), but below this depth the variation was minor. The inferred longer residence time of upwelled water over the shelf during earlier years would have also favored more O_2 consumption. It is also possible that the upwelling intensity is linked to the depth of source water from offshore OMZ; i.e., in 1958–1959 upwelling waters probably originated from the deeper part of the OMZ which is relatively cold and poorly ventilated. This clearly shows that the variable upwelling intensity between the periods resulted in the observed differences in O_2 saturations.

The stronger upwelling in 1959 has also displayed enrichment of midshelf nutrients in 1959 especially nitrate (1–25 μM) relative to 2012 (0.03–18.5 μM). About 10-fold higher subsurface nitrite maximum (10–20 m) during peak upwelling period in the past (~2 μM) than the present period shows higher nitrification potential in the early days which was also responsible for highly depleted O_2 conditions. Nevertheless, the varied nutrients enrichment enhances phytoplankton (Chl *a*) production which also exhibits interannual variation due to varying upwelling intensity.

5.2. Response of Inner Shelf to an Episodic Event

In early September 2012, an interesting feature occurred at station 4 (~35 km away from the coast). The water column had become much cooler, hypoxic (20%), and nutrient rich, but with low biomass (Chl *a*: 0.97 mg m^{-3}; zooplankton biomass: 0.88 ml m^{-3}). The adjacent inner shelf (stations 2 and 3) was, however, less saline (due to heavy precipitation for about 10 days prior to sampling) and O_2 supersaturated

(110–136%; Figure 14) with significantly high phytoplankton (Chl *a*: 5.6–11.6 mg m^{-3}) and zooplankton biomass (5.0–5.4 ml m^{-3}). This abnormal condition was not observed when we revisited the same location 4 days later. At this time there were media reports that most parts of beaches along the Kerala coast (southern part of SEAS), including Kochi, were completely exposed for 2 days (coinciding with the period of above abnormal feature), due to retrieval of seawater which was felt up to 35 km into the sea (see salinity distribution, Figure 14). Although presumably it was an eddy-mediated short-term event, such features have been noticed previously by the local residents. Under normal conditions, the upwelling waters would have advected up to coast, but in this instance the upwelled water was lifted to the surface at station 4. The resultant poor ventilation was adverse to most of the biological community so that the pelagic fishery moved away from this region to better ventilated waters of the inner shelf. The clustering of 60–80 fishing boats near station 3 and the absence of any boat near station 4 indicated that the latter site was not suitable for the fishes. Four days later when the area was revisited, typical monsoon upwelling conditions were reestablished with no signs of any abnormality.

5.3. Net Ecosystem Metabolism Over the Inner Shelf

$Chl_{p\text{-}int}$ did not show any correlation with either $GPP_{p\text{-}int}$ or $NPP_{p\text{-}int}$ (figure not shown), though the trend of $NPP_{p\text{-}int}$ variability was comparable with that of $Chl_{p\text{-}int}$ (Figure 10) suggesting that the environmental factors (light, nutrients, etc.) play a major role in regulating the primary production. Warm, calm, and oxic conditions during April and October–December facilitated the proliferation of cyanobacteria (*Trichodesmium erythreaum*), which constitute the second dominant microphytoplankton group after diatoms. Although the environmental conditions in April were comparable to those during November–December, the Chl *a* concentration during the former period was almost twice of that during the latter period (Figures 7 and 9a) as a result of relatively high nutrient concentrations through upwelling. Also, both seasons supported twofold higher bottom concentrations compared to surface as the entire water column was sun lit, the magnitude of former was higher by 30–50% than the latter. While the Chl *a* maximum at bottom during April has facilitated a twofold to threefold higher GPP compared to the surface, the same during November–December did not enhance the GPP (Figure 9c). The N/P ratio at the bottom was low during WM (3.0–4.5) as against a moderately higher ratio of 7 in April indicating substantial N limitation for GPP during the latter period. The low-surface NPP rate in July compared to June and September is also attributed to low N/P ratio.

The trophic status of the system will be net autotrophic if GPP/*R* is >1 and net heterotrophic if GPP/*R* is <1. Apart from light, N/P ratios also controlled the trophic status as low ratios (<10) witnessed autotrophy and high ratios (>10) heterotrophy (Figures 9f and 9g). The entire water column remained net autotrophic up to May, but with the onset of SM, it was restricted to surface layer below which, despite the nutrient enrichment, the system shifted to heterotrophy due to low GPP caused by light limitation and self-shading by phytoplankton. Also, the low O_2 concentrations could inhibit the growth of many phytoplankton. Despite significant drop in GPP rates, the column trophic status in October continued to follow the SM bimodal pattern of surface autotrophy and bottom heterotrophy. However, the trend reversed in November with heterotrophy in the upper 10 m and autotrophy below this depth. Following this, the column trophic status shifted completely to heterotrophy by December. The entire column GPP/*R* ratio shows that autotrophy prevailed from April (2.3) to May (2.5). Thereafter, the SM processes, mainly upwelling, made the system net heterotrophic during June–September (0.82–0.93). The October–December period was also characterized by net heterotrophy (0.33–0.61) albeit intense than SM due to very poor GPP. The annual mean GPP/*R* ratio was 1.11 ± 0.84 indicating that the inner shelf in 2012 was net autotrophic.

In order to check whether autotrophic production was sufficient to meet the respiratory demands, the excess bacterial demand (EBD) was calculated as follows:

$$\mathrm{EBD} = (\text{Column Community Respiration},\ R_{c\text{-}int}) - (\text{Photic zone GPP},\ GPP_{p\text{-}int})$$

The negative EBD during April–May (Figure 11) indicates net autotrophy following surplus organic production in the deep euphotic layer. However, the respiration increased from June to September to yield a positive EBD. The photic depth between SIM and SM was considerably reduced from about 100% to 30% of water column due to monsoon cloud cover and light shading by phytoplankton. Despite a greater than fourfold rise in surface Chl *a*, the photic column production during SM months did not vary significantly prior to onset of SM. At the same time, a twofold to threefold rise in respiratory demand of the increased dark compartment

(0 to ~70% of water column) between SIM and SM could not be met by the autotrophic supply that remained almost unchanged between these seasons. In the same manner, the EBD during WM was comparable with that of SM, despite a drop in production.

6. Conclusions

The Kochi time series of 2012 exhibited substantial intraannual variability in the biogeochemical properties in response to the combined effect of natural and anthropogenic activities. Upwelling is the dominant process controlling the biogeochemistry of SEAS on an annual basis. The present study provides the first detailed information concerning biogeochemical changes associated with the evolution, propagation, and decay of upwelling. Upwelling causes a drastic change from oligotrophic to nutrient-replete conditions leading to enhanced primary production during the summer monsoon. On an annual basis the inner shelf system was net autotrophic as the organic matter produced exceeded its consumption. The present O_2 saturations of Kochi midshelf waters during nonupwelling periods do not differ much from observations made five decades ago, but there was a marginal increase during the peak upwelling periods due to relatively weak upwelling in 2012. Although to the north of our study region along the west coast of India (approximately between Mangalore and Ratnagiri) the inner shelf has been experiencing sulphidic conditions [*Naqvi et al.,* 2006, 2009], such conditions do not seem to occur off Kochi presumably due to the difference in the initial oxygen content of upwelling source water. Our data do not show any indication of an intensification of hypoxic conditions due to human activities unlike many other coastal areas [*Diaz and Rosenberg*, 2008]. However, the low-oxygen subpycnocline waters over the shelf maintains the oxygen levels critically poised and just short of anoxia, underlining the vulnerability of the region to potential global change. In view of model results predicting the expansion of OMZs in the future [*Bopp et al.,* 2013], hypoxia in coastal waters of SEAS is expected to add further stress on coastal biogeochemistry and fishery resources.

Acknowledgments

The authors thank the Secretary, Ministry of Earth Sciences (MoES) for his support to this study. S.G.P. Matondkar, Shanta Nair, Mangesh Gauns, and Damodar Shenoy, NIO, Goa, have helped us in analyzing chlorophyll and ^{14}C samples. We are grateful to K. Banse, University of Washington, USA, for sharing the historical data and also providing constructive comments on the previous draft versions. The appreciations with positive comments of both the reviewers are greatly acknowledged. Thanks are also due to the FORV *Sagar Sampada* vessel management group for allotting the cruises and to the fishing hands and crew members for their onboard support during the cruises. The authors V.S., K.V.S., D.S., K.R.D., and G.L. thank the Centre for Marine Living Resources and Ecology, MoES for financial support. The data presented are archived at www.incois.gov.in. This work is undertaken as a part of the SIBER-India program of MoES.

References

Bakun, A., and R. H. Parrish (1982), Turbulence, transport and pelagic fish in the California and Peru Current systems, *Calif. Coop. Oceanic Fish. Invest. Rep.*, *23*, 99–112.

Balachandran, K. K., C. M. Laluraj, M. Nair, T. Joseph, P. Sheeba, and P. Venugopal (2005), Heavy metal accumulation in a flow restricted, tropical estuary, *Estuarine Coastal Shelf Sci.*, *65*, 361–370.

Balan, V. (1984), The Indian oil sardine: A review, *Mar. Fish. Inf. Serv. Tech. Ext. Ser.*, *60*, 1–10.

Banse, K. (1959), On upwelling and bottom-trawling off the southwest coast of India. *J. Mar. Biol. Assoc. India*, *1*, 33–49.

Banse, K. (1968), Hydrography of the Arabian Sea shelf of India and Pakistan and effects on demersal fishes, *Deep Sea Res.*, *15*, 45–79.

Bhavya, P. S., S. Kumar, G. V. M. Gupta, V. Sudheesh, K. V. Sudharma, D. S. Varrier, K. R. Dhanya, and N. Saravanane (2015), Nitrogen uptake dynamics in a tropical eutrophic estuary (Cochin, India) and adjacent coastal waters, *Estuaries Coasts*, doi:10.1007/s12237-015-9982-y.

Bopp, L., et al. (2013), Multiple stressors of ocean ecosystems in the 21st century: Projections with CMIP5 models, *Biogeosciences*, *10*, 6225–6245.

Bruce, J. G., D. R. Johnson, and J. C. Kindle (1994), Evidence for eddy formation in the eastern Arabian Sea during the northeast monsoon, *J. Geophys. Res.*, *99*, 7651–7664, doi:10.1029/94JC00035.

Central Marine Fisheries Research Institute (1964), Oceanographic station list, *Indian J. Fish.*, *A9*(1), 213–431.

Diaz, R. J., and R. Rosenberg (2008), Spreading dead zones and consequences for marine ecosystems, *Science*, *321*, 926–929.

Garcia, E. H., and L. I. Gordon (1992), Oxygen solubility in seawater: Better fitting equations, *Limnol. Oceanogr.*, *37*, 1307–1312.

Gardner, W., J. Gundersen, M. Richardson, and I. Walsh (1999), The role of seasonal and diel changes in mixed-layer depth on carbon and chlorophyll distributions in the Arabian Sea, *Deep Sea Res., Part II*, *46*, 1833–1858.

Grasshoff, K., M. Ehrhardt, and K. Kremling (Eds.) (1999), *Methods of Sea Water Analysis*, 3rd ed., pp. 75–89, 159–196, VCH, Wainheins, Germany.

Gupta, G. V. M., S. D. Thottathil, K. K. Balachandran, N. V. Madhu, P. Madeswaran, and S. Nair (2009), CO_2 supersaturation and net heterotrophy in a tropical estuary (Cochin, India): Influence of anthropogenic effect, *Ecosystems*, doi:10.1007/s10021-009-9280-2.

India Meteorological Department (2013), Monsoon 2012—A report, in *Met Monograph: Synoptic Meteorology No.13/2013*, edited by D. S. Pai and S. C. Bhan, pp. 36–46, Natl. Clim. Centre, India Meteorol. Dep., Pune, India.

Jabir, T., V. Dhanya, Y. Jesmi, M. P. Prabhakaran, N. Saravanane, G. V. M. Gupta, and A. A. M. Hatha (2013), Occurrence and distribution of a diatom-diazotrophic cyanobacteria association during a *Trichodesmium* bloom in the southeastern Arabian Sea, *Int. J. Oceanogr.*, doi:10.1155/2013/350594.

Jayaram, C., N. Chacko, K. Ajith Joseph, and A. N. Balchand (2010), Interannual variability of upwelling indices in the southeastern Arabian Sea: A satellite based study, *Ocean Sci. J.*, *45*(1), 27–40.

Johannessen, O. M., G. Subbaraju, and J. Blindheim (1987), Seasonal variations of the oceanographic conditions off the southwest coast of India during 1971–1975, *Fiskeridir. Skr., Ser. Havunders.*, *18*, 247–261.

Joint Global Ocean Flux Study (1994), Protocols for the Joint Global Ocean Flux Study (JGOFS) Core Measurements, IOC Manual and Guides, vol. 29, 119–122, 155–162, The United Nations Educational, Scientific and Cultural Organization (UNESCO), Paris.

Laws, E. A. (1991), Phytosynthetic quotients, new production and net community production in the open ocean, *Deep Sea Res., Part I*, *38*, 143–167.

Madhupratap, M., S. Prasanna Kumar, P. M. A. Bhattathiri, M. Dileep Kumar, S. Raghukumar, K. K. C. Nair, and N. Ramaiah (1996), Mechanism of the biological response to winter cooling in the northeastern Arabian Sea, *Nature*, *384*, 549–552.

Martin, G. D., P. A. Nisha, K. K. Balachdran, N. V. Madhu, M. Nair, P. Shaiju, T. Joseph, K. Srinivas, and G. V. M. Gupta (2010), Eutrophication induced changes in benthic community structure of a flow-restricted tropical estuary (Cochin backwaters), India, *Environ. Monit. Assess.*, doi:10.1007/s10661-010-1594-1.

Maya, M. V., S. G. Karapurkar, H. Naik, R. Roy, D. M. Shenoy, and S. W. A. Naqvi (2011), Intra-annual variability of carbon and nitrogen stable isotopes in suspended organic matter in waters of the western continental shelf of India, *Biogeosciences*, *8*, 3441–3456.

McCreary, J. P., P. K. Kundu, and R. L. Molinari (1993), A numerical investigation of dynamics, thermodynamics and mixed layer processes in the Indian Ocean, *Prog. Oceanogr.*, *31*, 181–244.

Menon, M. D., and K. C. George (1977), On the abundance of zooplankton along the south west coast of India during the year 1971–75, in *Proceedings of the Symposium on Warm Water Zooplankton*, *Spec. Publ.*, pp. 205–213, Natl. Inst. of Oceanogr., Goa, India.

Naqvi, S. W. A., and D. A. Jayakumar (2000), Ocean biogeochemistry and atmospheric composition: Significance of the Arabian Sea, *Curr. Sci.*, *78*, 289–299.

Naqvi, S. W. A., D. A. Jayakumar, P. V. Narvekar, H. Naik, V. V. S. S. Sarma, W. D'Souza, S. Joseph, and M. D. George (2000), Increased marine production of N_2O due to intensifying anoxia on the Indian continental shelf, *Nature*, *408*, 346–349.

Naqvi, S. W. A., H. W. Bange, S. W. Gibb, C. Goyet, A. D. Hatton, and R. C. Upstill-Goddard (2005), Biogeochemical ocean atmosphere transfers in the Arabian Sea, *Prog. Oceanogr.*, *65*, 116–144.

Naqvi, S. W. A., H. Naik, D. A. Jayakumar, M. S. Shailaja, and P. V. Narvekar (2006), Seasonal oxygen deficiency over the western continental shelf of India, in *Past and Present Water Column Anoxia*, edited by L. N. Neretin, pp. 195–224, Springer, Dordrecht, Netherlands.

Naqvi, S. W. A., H. Naik, D. A. Jayakumar, A. K. Pratihary, G. Narvenkar, S. Kurian, R. Agnihotri, M. S. Shailaja, and P. V. Narvekar (2009), Seasonal anoxia over the western Indian continental shelf, in *Indian Ocean Biogeochemical Processes and Ecological Variability*, *Geophys. Monogr. Ser.*, vol. 185, pp. 333–345, AGU, Washington, D. C.

Prasanna Kumar, S., M. Gauns, V. V. S. S. Sarma, P. M. Muraleedharan, S. Raghukumar, M. Dileep Kumar, and M. Madhupratap (2001), Physical forcing of biological productivity in the northern Arabian Sea during the northeast monsoon, *Deep Sea Res., Part II*, *48*, 1115–1126.

Rabalais, N. N., R. E. Turner, and W. J. Weisman Jr. (2001), Hypoxia in the Gulf of Mexico, *J. Environ. Qual.*, *30*, 320–329.

Rama Sastry, A. A., and P. Myrland (1959), Distribution of temperature, salinity and density in the Arabian Sea along the south Kerala coast (South India) during the post monsoon season, *Indian J. Fish.*, *6*, 223–255.

Rao, D. S., and C. P. Ramamirtham (1976), Seasonal variations in the hydrographical features along the west coast of India, *Indian J. Fish.*, *21*(2), 514–524.

Richard, H. F., J. C. James, and S. Vigg (1982), Secchi disc relationships, *Water Resour. Bull.*, *18*(1), 121–123.

Sarma, V. V. S. S., et al. (2009), Influence of river discharge on plankton metabolic rates in the tropical monsoon driven Godavari estuary, India, *Estuarine Coastal Shelf Sci.*, *85*, 515–524.

Sarma, V. V. S. S., V. R. Prasad, B. S. K. Kumar, K. Rajeev, B. M. M. Devi, N. P. C. Reddy, V. V. Sarma, and M. D. Kumar (2010), Intra-annual variability in nutrients in the Godavari estuary, India, *Cont. Shelf Res.*, *30*, 2005–2014.

Sarma, V. V. S. S., et al. (2013), Impact of atmospheric and physical forcings on biogeochemical cycling of dissolved oxygen and nutrients in the coastal Bay of Bengal, *J. Oceanogr.*, doi:10.1007/s10872-012-0168-y.

Schott, F. A., and J. P. McCreary Jr. (2001), The monsoon circulation of the Indian Ocean, *Prog. Oceanogr.*, *51*, 1–123.

Shalin, S., and K. V. Sanilkumar (2014), Variability of chlorophyll-a off the southwest coast of India, *Int. J. Remote Sens.*, *35*(14), 5420–5433.

Shankar, D., and S. R. Shetye (1997), On the dynamics of the Lakshadweep high and low in the southeastern Arabian Sea, *J. Geophys. Res.*, *102*, 12,551–12,562, doi:10.1029/97JC00465.

Shankar, D., P. Vinayachandran, and A. S. Unnikrishnan (2002), The monsoon currents in the north Indian Ocean, *Prog. Oceanogr.*, *52*, 63–120.

Sharma, G. S. (1978), Upwelling off the southwest coast of India, *Indian J. Mar. Sci.*, *7*, 209–218.

Shenoi, S. S. C., D. Shankar, and S. R. Shetye (1999), On the sea surface temperature high in the Lakshadweep sea before the onset of the southwest monsoon, *J. Geophys. Res.*, *104*, 15,703–15,712, doi:10.1029/1998JC900080.

Shenoi, S. S. C., D. Shanker, V. V. Gopalakrishna, and F. Durand (2005), Role of ocean in the genesis and annihilation of the core of the warm pool in the southeastern Arabian Sea, *Mausam*, *56*, 147–160.

Shetye, S. R., A. D. Gouveia, S. S. C. Shenoi, D. Sundar, G. S. Michael, A. M. Almeida, and K. Santanam (1990), Hydrography and the circulation off the west coast of India during southwest monsoon 1987, *J. Mar. Res.*, *48*, 359–378.

Thottathil, S. D., K. K. Balachandran, G. V. M. Gupta, N. V. Madhu, and S. Nair (2008), Influence of allochthonous input on autotrophic-heterotrophic switch-over in shallow waters of a tropical estuary (Cochin estuary), India, *Estuarine Coastal Shelf Sci.*, *78*, 551–562.

Wiggert, J. D., R. R. Hood, K. Banse, and J. C. Kindle (2005), Monsoon-driven biogeochemical processes in the Arabian Sea, *Prog. Oceanogr.*, *65*, 176–213.

Wong, G. T. F. (2012), Removal of nitrite interference in the Winkler determination of dissolved oxygen in seawater, *Mar. Chem.*, *130–131*, 28–32.